Materials Today Physics 59 (2025) 101897

Contents lists available at ScienceDirect

Materials Today Physics

journal homepage: www.journals.elsevier.com/materials-today-physics

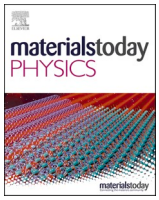

Edge state stabilization and control in 2D topological crystalline insulators

Chutian Wang [a,c], Yuefeng Yin [a,c,*], Thanh Tung Huynh [a], Michael S. Fuhrer [b,c], Nikhil V. Medhekar [a,c,**]

[a] Department of Materials Science and Engineering, Monash University, Clayton, VIC, Australia
[b] School of Physics and Astronomy, Monash University, Clayton, VIC, Australia
[c] ARC Centre of Excellence in Future Low Energy Electronics Technologies, Monash University, Clayton, VIC, Australia

A B S T R A C T

In a practical electronic device using a topological crystalline insulator (TCI), nontrivial topological states need to be stable against local perturbations while at the same time, allow for tuning via external controls such as an applied electric field. In this work, we use systematic first principles calculations to study the robustness of the topological states of planar bismuthene, a two-dimensional TCI. We show that the mirror symmetry-protected nontrivial topological phase can be maintained when the bismuthene monolayer has weak interactions with a substrate, or placed in a symmetry-protected heterostructure configuration. Our study also shows that edge terminations play an important role in modulating the electronic response of topological behaviours of 2D TCIs. We find that the edge states and the band gap for armchair edges become highly tunable with respect to modulated interfacial distance, symmetry, and external control means such as transverse electric field or pressure. These results provide guidelines for the selection of appropriate substrates for the experimental realization of TCI edge states, and could be useful for the design of novel electronic and spintronic devices.

1. Introduction

The recent progress in the field of two-dimensional (2D) quantum spin Hall Insulators points to a promising direction for developing future electronic and spintronic devices with low energy consumption [1]. A 2D quantum spin Hall Insulator is defined by its bulk-edge correspondence, where the bulk band topology can lead to the existence of topologically nontrivial spin-polarized helical edge states. These edge states are protected against non-magnetic perturbations such as disorder and backscattering as long as certain symmetries are preserved [2]. Although theoretical predictions have indicated that nontrivial band topology can exist in a wide range of materials [3], realizing the fabrication of topological devices still faces practical challenges. Of particular importance are the substrates, which act as support or contacts for 2D materials of interest in a typical device architecture. Substrates can also impart external fields that tune the band structure and alter the symmetry of the low-dimensional thin films deposited on it. A desirable 2D topological material therefore should have stable topological properties when interacting with substrates, in addition to a large enough band gap that is required to overcome the thermal energy at room temperature. Specifically for the applications in electronic transistors, it is required that the dissipationless topological edge current in a 2D topological material is conveniently switchable with a large on/off ratio [4–7]. These requirements pose critical challenges for identifying realistic topological materials used in low-energy electronic devices.

Recent experiments have demonstrated that topological edge states can be turned on and off through an external electrical field in a range of 2D or low-dimensional materials [4,8,9], for example, in Dirac semimetal Na_3Bi [10], quantum spin Hall Insulator Sb_2Te_3 [11], Weyl semiconductor Te [12] and topologically trivial ferromagnetic semiconductor $MnBi_2Te_4$ [13]. In these demonstrations, the applied external electric field changes the band ordering and either eliminates or induces the topological band inversion, thus changing the material's intrinsic topological nature [14,15]. However, for many topological systems, the degree to which bulk band gap can be manipulated using external fields is relatively limited. This has been the case for the materials such as bismuth bilayer (Bi (111)), for example, where electric field as large as 0.8 eV cause only slight change on its bulk band gap [16]. Moreover, the approach that relies on reordering of bulk band becomes much more difficult to implement in materials with a large intrinsic band gap, whifch are desirable candidates for room temperature application.

In contrast to band reordering, one alternative approach is to directly tune edge states of two-dimensional topological materials via symmetry breaking. In particular, topological crystalline insulators (TCIs) [17,18] offer an attractive prospect in this regard since the edge states of TCIs are protected by the combined effects of time reversal symmetry and

* Corresponding author. Department of Materials Science and Engineering, Monash University, Clayton, VIC, Australia.
** Corresponding author. Department of Materials Science and Engineering, Monash University, Clayton, VIC, Australia.
E-mail addresses: yuefeng.yin@monash.edu (Y. Yin), nikhil.medhekar@monash.edu (N.V. Medhekar).

https://doi.org/10.1016/j.mtphys.2025.101897
Received 13 January 2025; Received in revised form 24 September 2025; Accepted 14 October 2025
Available online 20 October 2025

crystalline symmetries. In principle, the topological edge states can be switched off if crystalline symmetries are broken in a TCI. Therefore, a high on/off operation speed can be expected, which makes TCI an attractive choice for high efficiency electronic devices [18,19]. Furthermore, TCI can be used to create novel transport patterns by manipulating its bulk-edge interactions [19]. Despite this promise, making electronic devices based on 2D TCIs is still a challenge since the conducting edge states ("on" state) are naturally tuned off due to breaking of the mirror symmetry induced by the underlying interacting substrates [20]. This emergent issue calls for a more systematic examination of substrate–film configurations to stabilize TCI materials while preserving the efficient switching behavior of the TCI channel in a FET setup.

Among the various materials that are being explored for topological transistors, allotropes of bismuth are promising due to their potential to have record-high band gaps and a large intrinsic spin-orbit coupling effect [21–24]. Bismuthene, a planar form of bismuth with hexagonal lattice, is a TCI with edge states protected by mirror symmetry [25]. However, these edge states are generally considered not robust and are sensitive to mirror symmetry-breaking [20]. Previous studies have found that placing bismuthene on SiC(0001) [21,26] and Ag (111) [27] will transform the material from a TCI to a Z_2 topological insulator due to the orbital filtering effect.

Motivated by the above mentioned experiments, we investigate whether the edge states in a TCI can—if at all—be maintained when in contact with substrates, and further, if such topological edge states on substrates can be tuned via external controls. Using monolayer bismuthene as an illustrative example of a TCI, we systematically employ first principles calculations and Wannier function-based tight binding models to explore the influence of various substrates on the topological edge states. We find that substrates like h-BN can be weakly interacting and TCI edge states can be maintained. In the case of strongly interacting

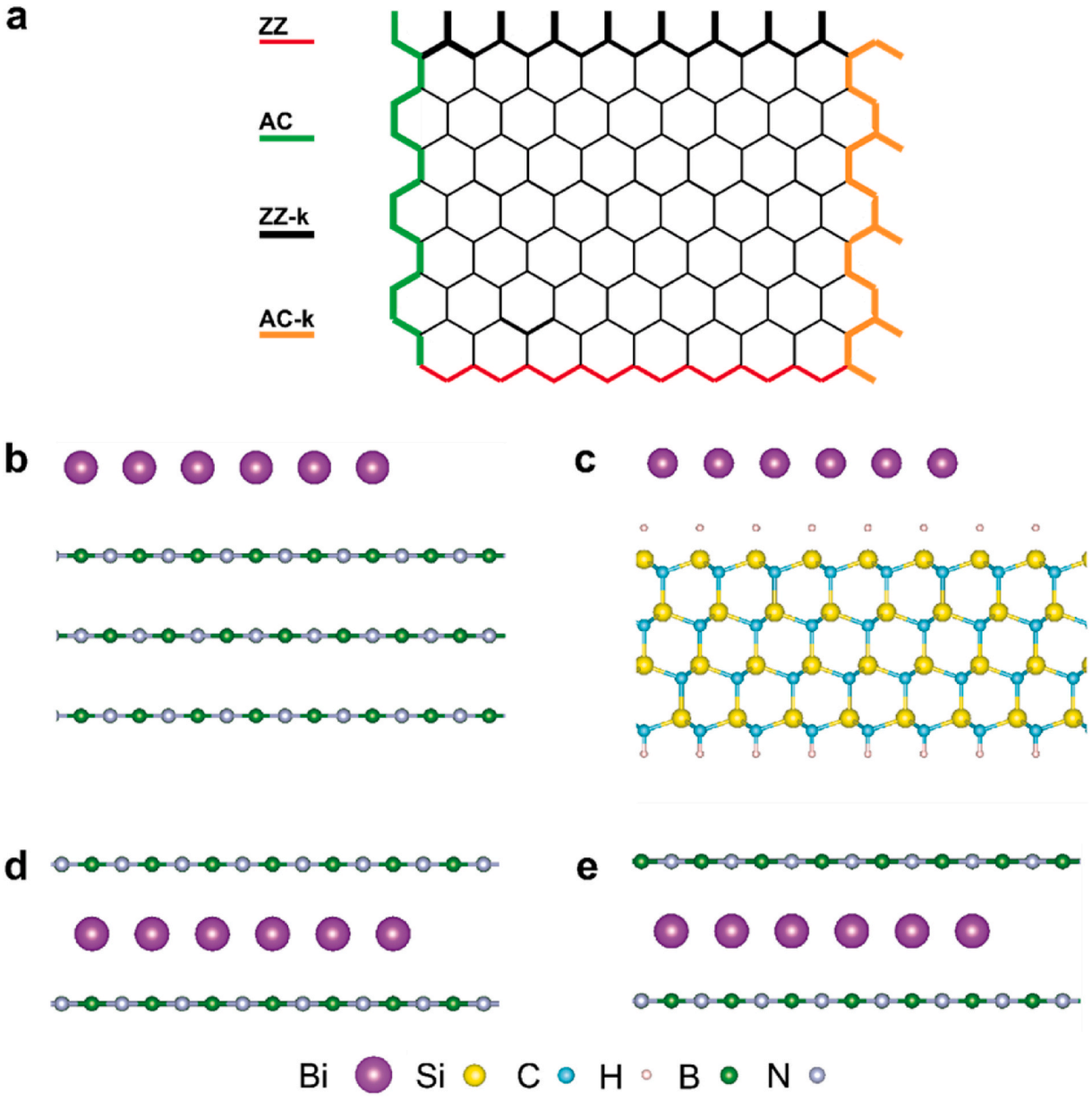

Fig. 1. Schematic for the configurations of 2D TCI bismuthene on substrates. **(a)** Different edge terminations of bismuthene: zigzag and armchair edges, pristine and with Klein defects with dangling bonds. **(b, c)** Bismuthene on h-BN and SiC-H(0001). **(d, e)** h-BN/bismuthene/h-BN sandwich structure. Only the h-BN layers nearest to the bismuthene monolayer are shown for clarity. The symmetry about the mirror plane passing through bismuthene layer is retained in **(d)**, whereas it is broken in **(e)** via a 60° rotation of the top h-BN layers with respect to the bottom h-BN layers.

substrates, the edge states can be protected via sandwich configurations that ensure mirror symmetry. Furthermore, these states can be conveniently tuned on/off by applying external controls knobs such as pressure and electric fields. We also show that with certain edge terminations, the spin filtered edge states of 2D TCI survive the mirror symmetry breaking fields, making it possible to achieve topological insulator-like phases on a strong mirror symmetry breaking substrate. Our results reaffirm that TCIs can be potential candidates for achieving a convenient switching of electronic states in nanodevices, as well as further suggest new approaches of tuning the edge states of topological materials.

1.1. Computational setup

Here we explore the edge states in monolayer bismuthene as an illustrative example of 2D TCI, both in its freestanding state and when supported on different substrates. We considered the typical zigzag (ZZ) and armchair (AC) edge terminations of bismuthene. In addition, to test how the edge states are influenced by the point defects present within the edges, we also considered the edge terminations with Klein defects, which introduce additional dangling bonds in the edge [28]. These edge terminations are denoted as ZZ-k and AC-k for the zigzag and armchair edge with Klein defects, respectively. The four edge terminations considered in our study are shown in Fig. 1(a). We examined interactions between these edge terminations with two different substrates, namely, hexagonal boron nitride (h-BN) and hydrogen passivated silicon carbide (SiC-H(0001), which are shown in Fig. 1(b) and (c) respectively. Both these substrates are considered as sufficiently inert substrates for group *V* materials [29]. The choice of these substrates is also motivated by a small lattice mismatch with bismuthene—the lattice constant for the relaxed, freestanding bismuthene is 5.27 Å, which closely matches a 2×2 surface unit cell of h-BN and a $\sqrt{3} \times \sqrt{3}$ R 30° surface unit cell of SiC-H(0001) (surface lattice parameters of 5.02 Å and 5.34 Å, respectively). Both these substrates thus induce a strain smaller than 5 % in bismuthene. This magnitude of strain between bismuth and the underlying substrate can be realized experimentally by encapsulation, gradual deposition, and application of external pressure. Several studies have reported using SiC–H(0001) and h-BN to guide the growth of various low-dimensional bismuth structures, and similar strategies may be applicable to the growth of planar bismuthene [23, 30].

2. Results and discussions

2.1. Freestanding bismuthene

We first revisit the electronic structure of freestanding, planar bismuthene. In its freestanding form, bismuthene is predicted to be a topological crystalline insulator with edge states protected by mirror symmetry [31]. Fig. 2 shows the calculated electronic band structures of bismuthene and bismuthene nanoribbons. Our calculated band structures for planar bismuthene (Fig. 2(a)), as well as nanoribbons with ZZ (Fig. 2(b) and (d)), and AC (Fig. 2(c) and (e)) terminations are consistent with previously published DFT and tight-binding results [24,25]. We can clearly see observe edge states in Fig. 2(b–d) continuously connecting the top of the valence band and the bottom of the conduction band. We

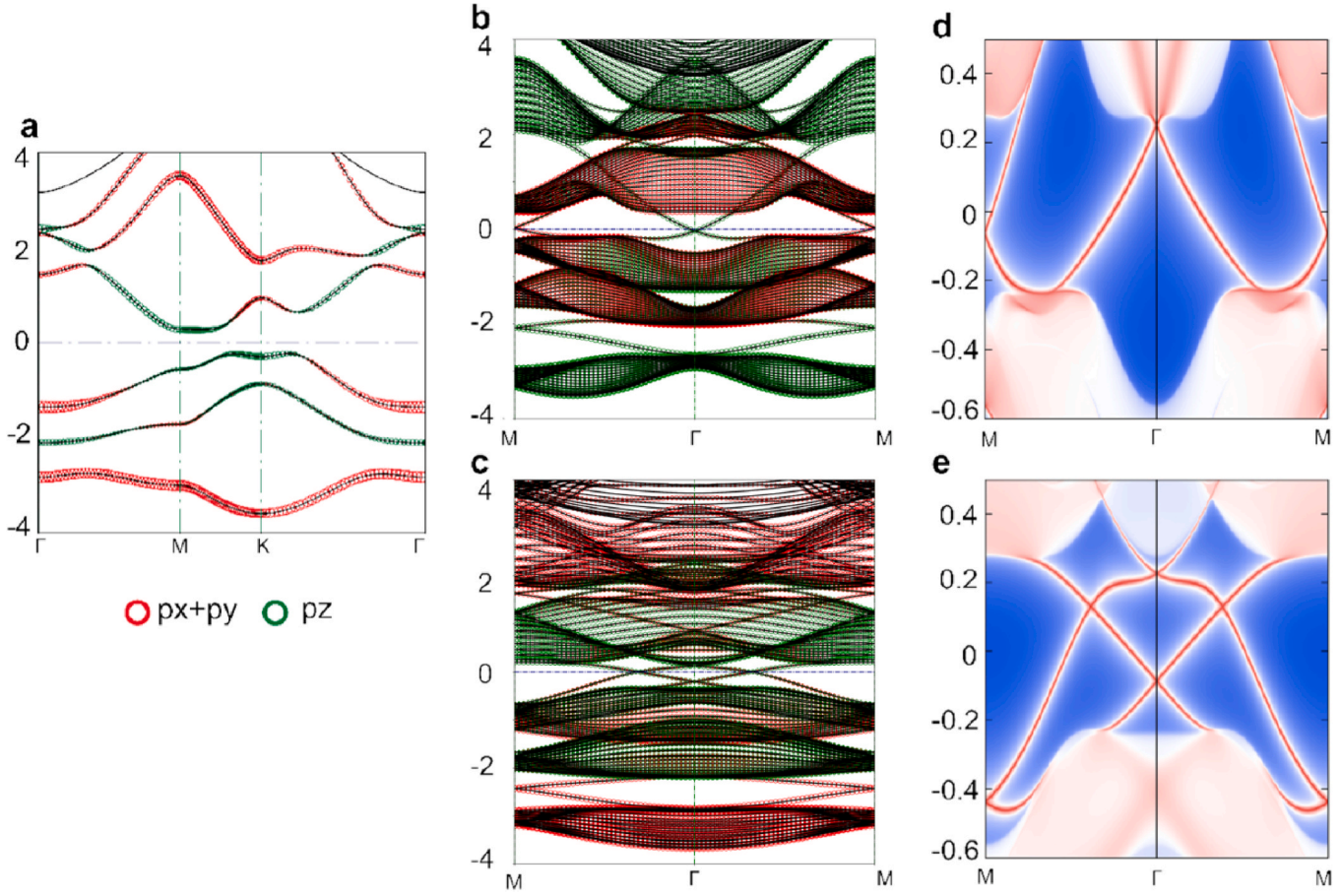

Fig. 2. Electronic band structures with orbital projection obtained using first principles density functional theory calculations. (a) Freestanding bismuthene, **(b)** ZZ nanoribbon, and **(c)** AC nanoribbon. **(d–e)** Wannier projections onto ZZ and AC edge terminations, respectively. All energies are relative to the Fermi level.

have verified that freestanding bismuthene has a mirror Chern number of 2 via Wannier tight-binding methods, confirming it to be a TCI.

We also calculate the orbital characters of bands as shown in coloured circles in Fig. 2(a–c). These orbital characters will be useful later to illustrate the change in electronic and topological properties due to interaction with substrates. For freestanding bismuthene, we can observe the features of band inversion between $px + py$ (red) and p_z (green) orbitals at TRIM (time reversal invariant momenta) K. As a result of this band inversion, edge states in bismuthene nanoribbons in Fig. 2 (b–e) form inside the gapped region connecting the valence band with the conduction band. We have also found that different edge terminations lead to different edge band degeneracy features and orbital characters. Zigzag nanoribbons (Fig. 2(b) and (d)) show edge band degeneracy point at Γ contributed by $px + py$ orbitals, while the degeneracy at M is dominated by p_z orbitals. However, for armchair (Fig. 2 (c) and (e)), AC-k and ZZ-k (Fig. 3) edge terminations, the edge band crossings are located at generic kpoints, with combined $px + p_y$ and p_z orbital characters.

2.2. Bismuthene on SiC-H(0001)

We first examine the interaction between bismuthene and silicon carbide (SiC), a popular choice as the supporting substrate for bismuthene. Previous reports have shown that bismuthene can bind covalently to SiC [21,26,32,33]. However, the formation of covalent bonds between bismuthene and the substrate turns the bismuthene into a Z2 topological insulator [21]. Therefore, to preserve the TCI nature of bismuthene when placed on a substrate, we have passivated of the SiC (0001) surface with hydrogen atoms to form a nearly inert substrate denoted as SiC-H(0001). The interaction between bismuthene and SiC-H (0001) is now mainly governed by weak van der Waals forces, with the van der Waals gap between fully relaxed bismuthene and the substrate being 4.8 Å. Hence the electronic structure of bismuthene can be expected to be significnatly less perturbed by the SiC-H(0001) substrate compared to the covalent-bonded substrate.

We first assess the thermodynamic stability of bismuthene on SiC-H (0001) substrate by calculating the cohesive energy. The cohesive energy is defined as $E_c = E_{tot} - E_{sub} - N \times E_{Bi}$, where E_{sub} is the energy of the relaxed SiC-H(0001) substrate slab, E_{Bi} is the per atom chemical potential of bismuth in its gas phase single atom form, and E_{tot} is the total energy of the bismuthene-substrate system. A negative E_c value means that formation of a bismuthene layer on a substrate is energetically favorable. We find that the cohesive energy of bismuthene on SiC-H (0001) is −2.01 eV/atom, which is much higher compared to −4.00 eV/atom on covalently-bonded SiC-(0001) substrate, indicating that bismuthene does not form strong covalent bonds with the underlying hydrogen-terminated SiC-H(0001) substrate, but still energetically favorable. The strength of these weaker interactions between bismuthene and the substrate can be estimated by the binding energy, calculated as $E_b = E_{total} - E_{sub} - E_{bismuthene}$, where $E_{bismuthene}$ is the energy of relaxed thin film bismuthene. We find that the binding energy for bismuthene on SiC-H(0001) is −0.14 eV/atom, which is within the range for van der Waals interactions [34], indicating a weaker interaction compared to covalently-bonded planar bismuthene SiC-(0001) substrate (−2.21 eV/atom).

We next calculate the edge band structure of bismuthene nanoribbons on a SiC-H(0001) substrate with all terminations considered using Wannier-based tight-binding models as shown in Fig. 3(a–d). In general, similar to the freestanding bismuthene, we can observe two branches of edge bands around the Fermi level. The influence of the sustrate on the edge states depends strongly on edge configurations. For AC and AC-k edges, the edge band degeneracies along $\bar{\Gamma} - \bar{M}$ are broken (highlighted by circles in Fig. 3(b–d)), suggesting the substrate has switched off the TCI phase in bismuthene. However, the edge band degeneracies for ZZ (Fig. 3(a)) and ZZ-k (Fig. 3(c)) edges are maintained. For the ZZ edge, this is due to the fact that band degeneracies are located at TRIM points, thus stabilized by the presence of time-reversal symmetry. We can find that the degeneracies can only be broken if they are at generic k points, instead of TRIM, which becomes the main factor alters the band topology of TCI for when the edge configuration is different. It should be noted that although degeneracies at generic band crossing kpoints at ~0.4 eV energy in ZZ-k edge are not broken as seen in

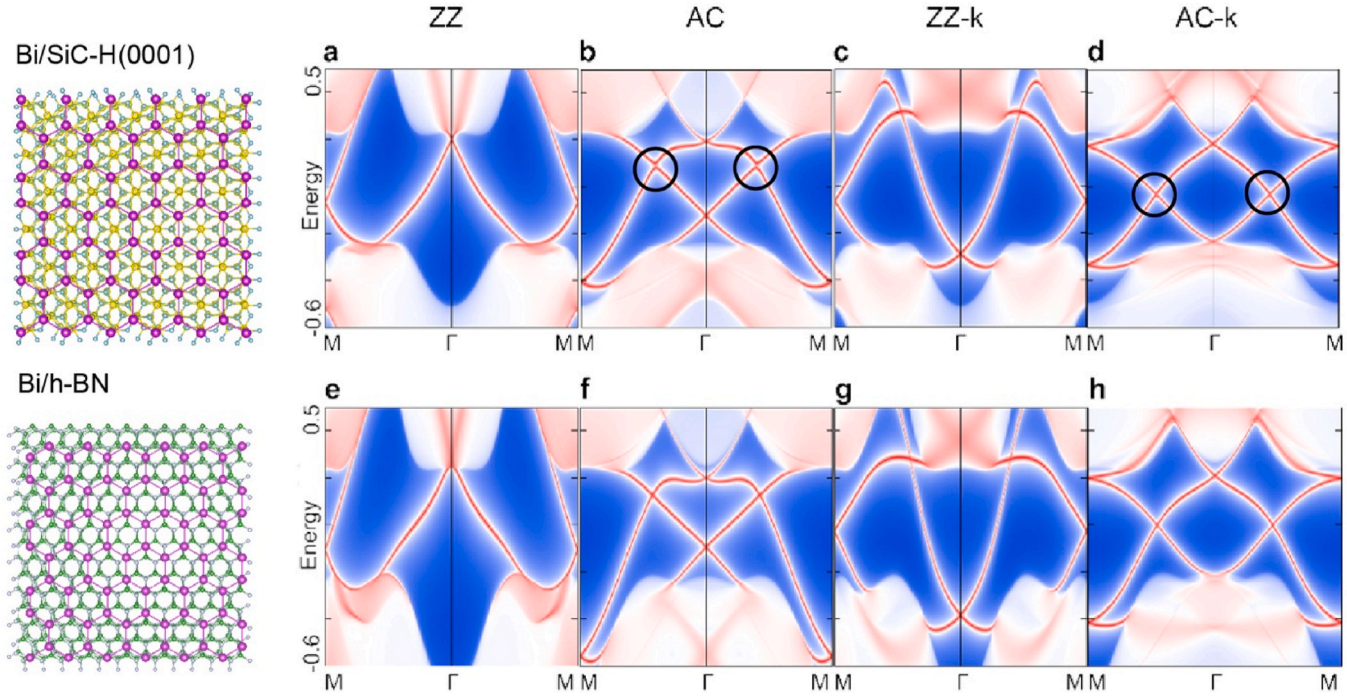

Fig. 3. Wannier edge band dispersions for bismuthene on (a–d) SiC-H(0001) and (e–f) h-BN substrates. (a, e) ZZ edge, **(b, f)** AC edge, **(c, g)** ZZ-k edge, and **(d, h)** AC-k edge. Black circles in (b, d) denote the degeneracy breaking points. The left graph demonstrates the equivalent nanoribbon model with AC edge. All energies are relative to the Fermi level.

Fig. 3 (c), as we show later, these degeneracies are sensisitve to transverse pressure and can be broken with sufficient applied pressure (see Fig. 5 and the associated discussion).

2.3. Bismuthene on h-BN

Next we investigate the interaction of bismuthene with another wide bandgap semiconducting substrate, h-BN. The van der Waals gap between fully relaxed bismuthene and the substrate is 3.8 Å, smaller than the SiC-H(0001) substrate. The cohesive energy of bismuthene on h-BN is −1.86 eV/atom, and the binding energy is −0.06 eV/atom, indicating that the interaction between bismuthene and h-BN is much weaker than that between bismuthene and SiC–H(0001). (For a discussion on the dynamic stability of the structure, see the phonon band structure in Supplementary Note 1 and Fig. S1.) The edge band structure of bismutene nanoribbons on h-BN is shown in Fig. 3(e–h). We find that the edge band dispersion is nearly unaffected for all edge configurations when compared to freestanding bismuthene. The edge states are still gapless, suggesting that TCI states are still protected. This is noteworthy since the van der Waals gap between bismuthene and the substrate is smaller for h-BN substrate compared with SiC-H(0001) substrate. Therefore we can conclude that if the interaction between the bismuthene and the substrate is weak enough, the TCI states of bismuthene can still be maintained and stabilized.

A few previous studies have reported that h-BN can lead to broken edge band degeneracies in bismuthene [31]. This can be explained by the narrow width (~3 nm) of the nanoribbons used in these studies. A topologically trivial gap can open in a nanoribbondue to the interactions between two edges, and this effect becomes more evident as the width of the nanoribbon decreases [35]. We have confirmed this via a similar DFT analysis using a nanoribbon of sub 3 nm width. We find edge band degeneracies are broken even for a freestanding bismuthene. These results can in turn indicate that the edge states can be fragile against size effects, but should be robust against weak substrate perturbations.

We also performed HSE06 calculations [36] for the edge band structures of bismuthene nanoribbons on both SiC–H(0001) and h-BN substrates to address the band-gap underestimation in GGA-PBE. The 2D bulk band structures show an increase of ~0.1 eV with HSE06 relative to GGA-PBE, with negligible changes in band geometry (Fig. S2). For the edge band structures (Fig. S3), the HSE06 results are nearly identical to those obtained with GGA-PBE, preserving all qualitative features across the different edge terminations. Specifically, for bismuthene on SiC–H (0001), the breaking of degeneracies for AC and AC-k edges and the preservation of degeneracies for ZZ and ZZ-k edges remain unchanged; by contrast, for bismuthene on h-BN, the edge states remain gapless, and the TCI features are fully maintained. The only quantitative difference with GGA-PBE results is a slight numerical change in the edge band gap value. These results have demonstrated consistence with our observations from the GGA-PBE calculations.

2.4. Substrate/bismuthene/substrate sandwich heterostructure

We have shown that the weak van der Waals interaction imposed by substrates such as h-BN can preserve the TCI states of planar bismuthene. However, such a one-side stacking approach is not a convenient way to protect the TCI phase of planar bismuthene since the in-plane mirror symmetry can be easily broken if the perturbations from the substrate are strong enough. In practice, stabilization of TCI edge states would therefore require a delicate control of the interaction between bismuthene and the substrate interaction. Alternatively, we can take the advantage of using these van der Waals systems to achieve an efficient and flexible control of the interfacial contact.

Here we propose a new heterostructure by placing the bismuthene sandwiched between h-BN layers. This sandwiched configuration of h-BN layers is designed in such a way that the mirror symmetry of bismuthene layer is protected, whereby the edge states of bismuthene can survive the interactions with substrates. We have confirmed this by calculating both zigzag and armchair edge states (not shown here), which illustrate that degeneracies in edge band structures—similar to those shown in Fig. 3(e and f)—are preserved. On the other hand, when the mirror symmetry is broken via a 60° rotation of the h-BN layers on one side of bismuthene with respect to the other side as shown in Fig. 1 (a), bismuthene becomes topologically trivial with gaps opening at generic *k* points for AC and AC-k edges as expected. These results suggest that it is possible to protect the edge states of TCI by constructing an appropriate stacking of the TCI layer and substrates on either side. As we illustrate next, such controlled stacking also allows us to further modify the electronic response of the TCI layer.

2.5. Controlling armchair edge band gap via interfacial van der waals gap

We next investigate whether the interfacial contact between bismuthene and substrates—and thereby the edge states in bismuthene—can be modified by reducing the interfacial distance via external pressure. In Fig. 3, we have seen that armchair edges are more susceptible to the influence from the substrates, especially at generic *k* points in the Brillouin zone. Therefore, we calculate the evolution of the armchair edge band gap in bismuthene nanoribbons supported on substrates as a function of the pressure as presented in Fig. 4. For a comparison, we also show the calculated 2D bulk bandgap of bismuthene on the same substrates. In the case of SiC-H(0001) (Fig. 4(a)), when the interfacial distance is reduced from the relaxed distance of 4.8 Å, the band gap in the 2D band structure of bismuthene gradually decreases. In the corresponding edge band structure for the armchair bismuthenne nanoribbons on SiC-H(0001), the edge gap opens and becomes larger as the van der Waals interfacial distance decreases. Note two distinct values for the edge gap since the two armchair edges on SiC-H(0001) are not equivalent due to the crystal symmetry of the substrate. In Fig. 5(a–d), we show the edge band dispersion of bismuthene on SiC-H(0001) with a reduced van der Waals interfacial distance of 3.8 Å as indicated by the dashed in Fig. 4(a). It can be observed that the edge band degeneracies are broken at non-TRIM points along $\overline{\Gamma} - \overline{M}$ for AC, AC-k and ZZ-k edge configurations. These observations imply that reduced interfacial distance induces a strong mirror symmetry-breaking potential.

We can observe a similar trend if the supporting substrate is h-BN as shown in Fig. 4(b). Here we have considered two configurations presented in Fig. 1, namely, where bismuthene is supported on h-BN on one side (Fig. 1(b)) and where bismuthene is sandwiched between h-BN substrate on both side such that the mirror symmetry is broken via ia a 60° rotation of the top h-BN layers with respect to the bottom h-BN layers (Figure (1e)). Earlier, we have shown that the TCI phase of bismuthene is preserved at a relaxed distance (3.8 Å). When the interfacial distance is reduced via external pressure, the influence of the substrate on the electronic structure of bismuthene becomes more significant and breaks the edge degeneracies protected by the mirror symmetry. This is reflected in the armchair edge dispersion on h-BN substrate with a compressed van der Waals gap of 2.9 Å as shown in Fig. 5(f). The edge band gap reaches a maximum of 210 meV for the sandwich heterostructure at the interfacial van der Waals gap of 2.75 Å. Upon subsequent compression, the edge band gap begins to decrease, approaching nearly zero at 2.3 Å. As we discuss later, this variation in the edge band gap in bismuthene on h-BN is a result of the competing mechanism between the mirror symmetry breaking potential which drives the opening of edge band gap and the closing of the 2D bulk a s a consequence of the reduced interfacial distance.

In summary, we can oberve that tuning the interfacial distance between bismuthene and the substrate is effective in switching the intrinsic topological nature of TCI bismuthene. In experimental setup, this can be achieved by applying external pressure (e.g. hydrostatic pressure) and encapsulation to enforce a closer interfacial contact [37]. We can estimate the relationship between the interfacial distance *d* and the

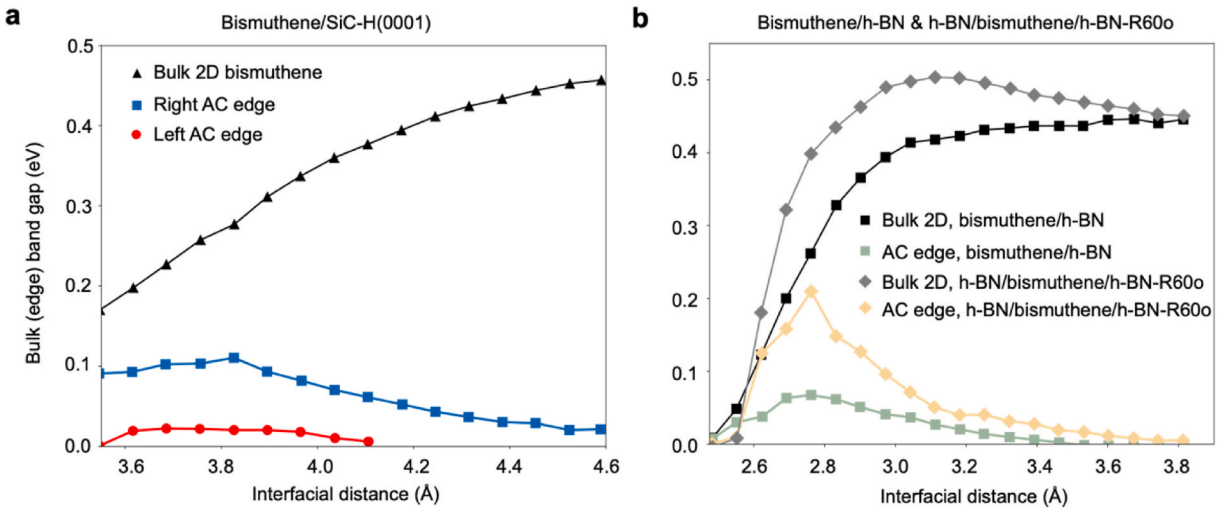

Fig. 4. The evolution of edge band gap in bismuthene armchair nanoribbon on (a) SiC-H(0001) and (b) h-BN substrate with interfacial distance. The 2D bulk band gap of bismuthene on the same substrates are also shown for comparison. In (a), the two armchair edges of bismuthene on SiC-H(0001) are not equivalent. In (b), edge and bulk band gaps for armchair bismuthene are also reported for mirror-symmetry broken sandwiched heterostructure, where top h-BN layers are rotated 60° with respect to the bottom h-BN layers.

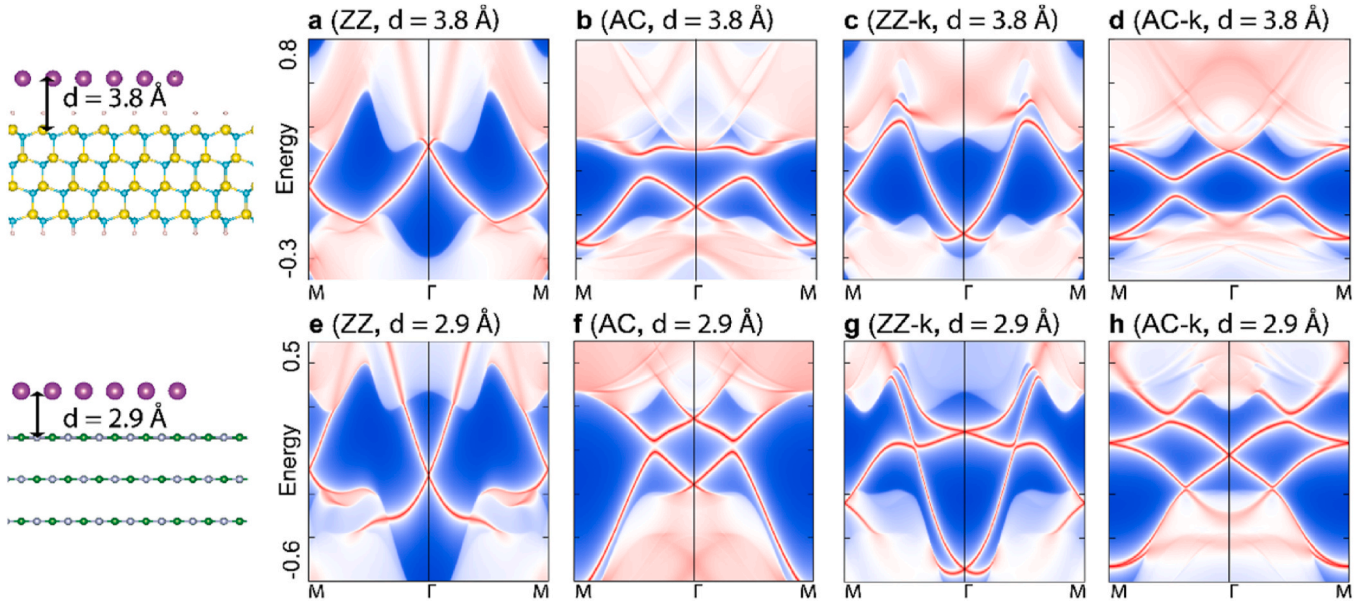

Fig. 5. | Influence of reduced van der Waals interfacial distance on edge band dispersions for bismuthene on (a–d) SiC-H(0001) and (e–f) h-BN substrates. (a, e) ZZ edge, **(b, f)** AC edge, **(c, g)** ZZ-k edge, and **(d, h)** AC-k edge. The van der Waals interfacial gap is compressed to 3.8 Å and 2.9 Å for SiC-H(0001) and h-BN substrate, respectively. All energies are relative to the Fermi level.

interfacial pressure P as $P = \frac{\partial E}{\partial d}/A$, where E is the total energy of the bismuthene-substrate system as calculated from DFT. We have plotted the evolution of band gaps as a function of the estimated interfacial pressure in Fig. S4. As expected, the pressure required to achieve maximum edge band gap depends on the substrate, from ~7 GPa for SiC-H(0001) to 30 GPa for h-BN to achieve a similar maximum edge band gap.

It is worth noting that the intrinsic topological nature of bismuthene in a hBN/bismuthene/hBN sandwich heterostructure remains protected even at much reduced van der Waals interfacial gaps. We have tested this by calculating the edge band structures of bismuthene at an interfacial gap of 2.9 Å (compressed by 1 Å from the relaxed distance) as shown in Figure S5 (a-d). It can be observed that the edge band degeneracies are preserved, meaning that although applying external pressure can induce significant influences on the electronic structure of bismuthene, its topological nature can still be preserved as long as the mirror symmetry is maintained. Once the symmetry is broken via a 60 ° rotation of h-BN on one side of bismuthene relative to other (Figure S5 (e-h)), the applied external pressure strongly influences both the 2D bulk and edge band gaps in this configuration.

2.6. *The effect of edge configurations*

Next we discuss how the electronic structure of bismuthene nanoribbons can be affected by the configuration of edge terminations. The interplay between the substrate potential and the edge structure can lead to different electronic responses in the edge states (see Figs. 3 and 5). For ZZ-k, AC and AC-k edges, the energy degeneracies in the edge bands are only broken at generic k points, while the degeneracies at high symmetry points are retained. However, for the ZZ edge, degeneracies

only occur in the high symmetry points Γ and M. Consequently, we do not observe breaking of degeneracies even when strong pressure/rotation effects are applied. These results can be explained by that degeneracies at those time reversal invariant momenta (TRIM) pointsare protected by time reversal symmetry, while the degeneracy at other generic kpoints are not. Since ZZ edges only have edge states connecting at TRIM near the Fermi level, the edge states can then survive strong substrate effects that do not break time reversal symmetry.

The robustness of the ZZ edge can also be explained by the separation of p orbital characters in the edge bands. Previous studies have suggested that the electronic bands of planar bismuthene near the Fermi level are composed of two branches of topologically nontrivial bands with $px + p_y$ and p_z character, respectively [21,38]. However, the combination of these bands leads to a trivial Z_2 band topology. Considering this, and by analysing the character of edge bands, we find that ZZ edges, unlike armchair terminations, have completely separated $px + p_y$ and p_z bands. As shown in Fig. 2(b), the orbital character near Γ is dominated by $px + p_y$, while the p_z orbital is concentrated near M for ZZ edges. While for AC and ZZ-k terminations, the $px + p_y$and p_z orbitals are all mixed together on the edge bands (Fig. 2(c) and (d)). Therefore if the mirror symmetry of the nanoribbon is broken by substrates or external factors, the edge degeneracies at non-TRIM positions (Γ or M) with all p orbitals mixed will not be protected for AC and ZZ-k edges. (for e.g., Fig. 5(b)(c)). The edge degeneracies in ZZ nanoribbon only occur at TRIM points and they should be robust against mirror symmetry perturbations which can not be broken as long as the time reversal symmetry is conserved.

Finally, the two separated branches at Γ and M in the zigzag nanoribbon can be bridged if we can induce structural defects such as forming the Klein defects at edges, i.e. ZZ-k edge terminations. The edge bands in ZZ-k nanoribbons consist two separated band approaches centring at Γ and M. However, with the change of edge band energy alignment, the two branches now have an additional degeneracy along Γ − M, The p orbital characters become mixed near this band degeneracy, as in the case of AC and AC-k nanoribbons. When the mirror symmetry is lifted, the edge degeneracies are broken and a band gap appears. Indicate that the stability of edge states in a TCI depends not only whether the mirror symmetry of the TCI lattice is broken, but also by the position of the edge band degeneracies and the band orbital characters. As shown in a recent study, this effect can be effectively exploited to selectively tune the edge currents in TCI with different edge terminations [19].

Edge-state modulation by Klein defects (–k nanoribbons) clearly demonstrates how edge dispersion depends on termination. Although uniform Klein edges have rarely been observed experimentally, traces of Klein defects have appeared when 2D edges are exposed to small gas molecules or ion irradiation [39]. Our results are qualitatively consistent with previous results for 2D Bi(111), in which Klein edges substantially reshape the edge-state dispersion [40]. Specifically, we show that Klein edges strengthen bulk–edge hybridization, increase entanglement between edge branches, and generate new edge degeneracies at generic k points. We can further suggest that, at the low Klein-defect concentrations, ZZ edge states should still exhibit measurable shifts in degeneracy energies and the emergence of additional degeneracies. Overall, the Klein defect results highlight the robustness of bulk–edge correspondence in TCIs and motivate experimental designs for new edge-tuning strategies.

2.7. Wannier charge center analysis

We next evaluate topological invariants of the various bismuthene-substrate systems considered here by calculating the evolution of Wannier charge center (WCC) evolution. As shown in Fig. S6, we can infer that the Z_2 number of bismuthene on all substrates is 0. In cases, where the perturbations from the substrate are weak (for example, bismuthene on h-BN, Fig. S6(a)), or where the mirror symmetry is enforced (for example, h-BN/bismuthene/h-BN heterostructure, Fig. S6(c)), the WCC evolution graph shows two branches of WCC lines connecting along $k = 0$ to $k = \pi$, consistent with the mirror Chern number of 2. The connections along the [0, π] corresponds to the location of the mirror-symmetry protected degeneracies. For the scenarios involving mirror symmetry-breaking perturbation such as bismuthene/SiCH-0001 (Fig. S6(b)), bismuthene under pressure (Fig. S6(d)), or mirror symmetry broken h-BN/bismuthene/h-BN-R60° heterostructure (Fig. S6 (e)), we observe a disconnect in the WCC lines on [0, π], indicating that the TCI phase is broken [41]. These results have show substrates with weak interactions and sandwiched heterostructures enforcing mirror symmetry can potentially be used as a good platform to achieve protected edge states in TCIs, and furthermore, tuning their interfacial contact can effectively switch on/off the TCI phase for its applications in transistor devices.

2.8. Effective tight-binding Hamiltonian model of bismuthene on substrates

To gain deeper insights into the origins of the effect of weak perturbations on the electronic structure of bismuthene nanoribbons, we have built a simple, second-nearest neighbor tight-binding model for freestanding bismuthene nanoribbon based on Wannier projections from DFT calculations [38]. The tight-binding Hamiltonian can be expressed as $H = t\sum_{\langle ij\rangle} c_i^{\dagger} c_j + \lambda_{SO}\mathrm{L}\cdot\mathrm{S}$ where the first term represents hooping between neighboring bismuth atoms with hopping strength t and the second term represents the intrinsic spin-orbit coupling of bismuth with a spin-orbit coupling strength of $\lambda_{SO.}$ As shown in Fig. 6, the band structures obtained using this tight binding model show a a good agreement with DFT results for ZZ and AC nanoribbons presented in Fig. 1. Following the examples in Ref. [42] to model the effect of interactions with substrates or a transverse electric field, we have added the following Rashba term to our Tight Binding Hamiltonian $H_R = \lambda_R \psi \sum_i c_i^{\dagger} \sigma_x \tau_z s_y - \sigma_y s_x c_i$ [35]. Fig. 6 also shows the evolution of the band structures with increasing symmetry-breaking Rashba parameter $\lambda_{R.}$ The model is consistent with our results presented earlier, showing that the substrate effect can be appropriately demonstrated by mirror symmetry breaking factors such as the Rashba parameter.

We can now estimate the magnitude of the transverse electrical field E corresponding to the symmetry-breaking Rashba parameter λ_R using the relationship $\lambda_R = \frac{eEz_0}{3(sp\sigma)}\varepsilon$ [36]. Here, the Slater-Koster matrix element $sp\sigma = 1.3$ for bismuth [43] and the spin orbit strength $\varepsilon = 1.158$. As shown in Fig. S7, the edge band gap in AC nanoribbons increases with increasing Electric field E before reaching a maximum. The maximum edge band gap of approximately 120 meV is obtained at a Rashba parameter of $\lambda_R = 0.15$ or a transverse electric field of 1.75 V/nm. This band gap is significantly larger than the thermal energy of around 25 meV at room temperature, making it sufficient to mitigate the effects of thermal excitation. The relatively large band gap suggests enhanced stability and efficiency in maintaining control over electron dynamics at room temperature, which could improve power efficiency and switching performance in related applications.

2.9. Implications to other TCIs

While our investigations and proposed setups are focused on the 2D TCI bismuthene, these results should also have general implications for fully realizing the potential of TCIs. (Pb,Sn)Te has been the most widely studied TCI system so far. Despite numerous theoretical predictions and claimed experimental syntheses [18,44,45], the (Pb,Sn)Te system has not been fully regarded as a viable TCI platform. The primary reason is the challenge of obtaining high-quality and stable (Pb,Sn)Te crystals in experiments that can exhibit TCI features. The symmetry-protected TCI character can be easily transformed into a trivial electronic structure or other topologically nontrivial phases (e.g., a topological insulator)

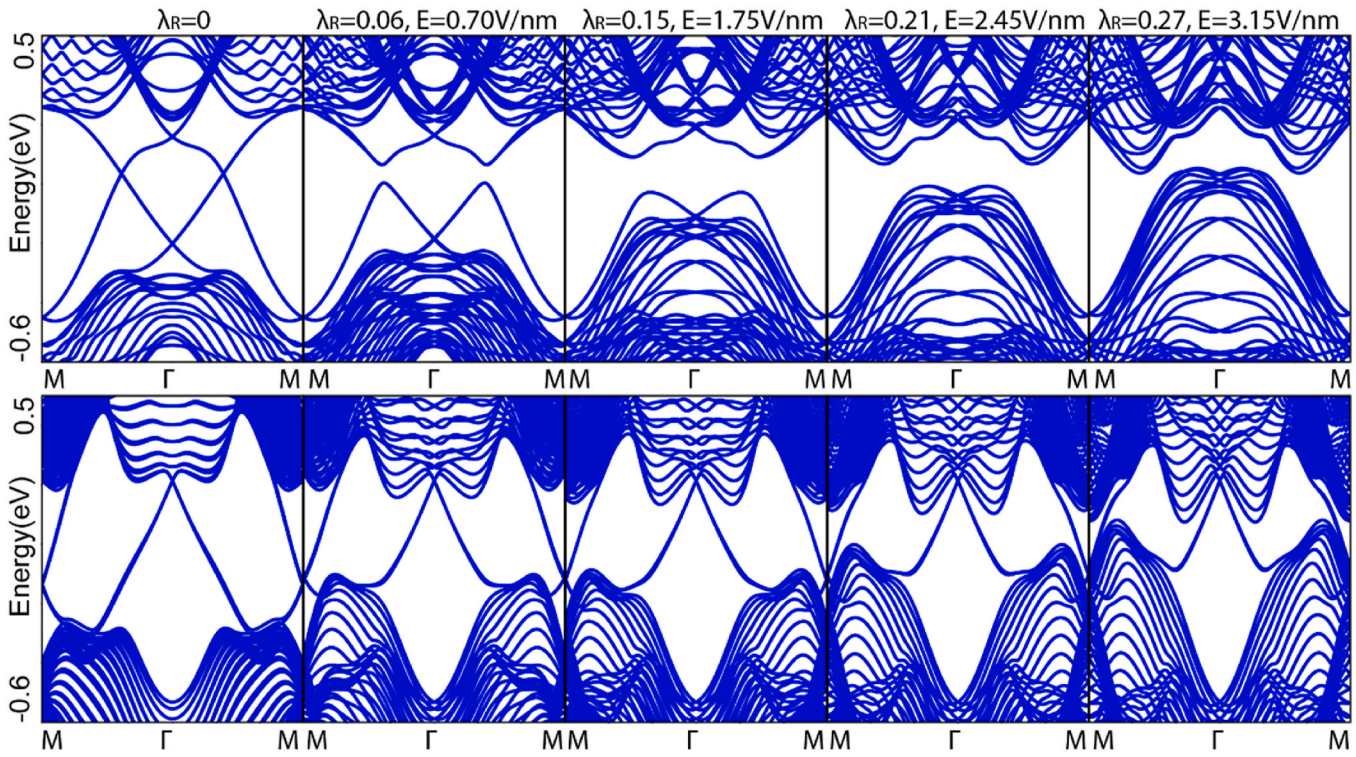

Fig. 6. Evolution of band structures of AC (top) and ZZ (bottom) bismuthene nanoribbons calculated using effective tight binding Hamiltonian with the Rashba parameter λ_R or the effective electric field (in arbitrary energy units).

under the influence of substrate interactions, strain, or doping [46]. The fragility of the TCI states in the (Pb,Sn)Te system is also reflected in the challenge of experimentally observing the conducting TCI surface states [47,48]. Due to symmetry reductions and surface reconstructions, it is not clear whether all surface states observed in the (Pb,Sn)Te system are of TCI nature.

Compared to (Pb,Sn)Te, bismuthene is a better choice for realizing the promising potentials of TCI. First, the bulk band gap of bismuthene (~0.8 eV) is much larger than that of (Pb,Sn)Te (~0.3 eV) [49], making it a better choice in semiconductor applications. Moreover, because the structure is reduced to 2D, it is much easier to judge the nature of protection for bismuthene's edge states compared to the (Pb,Sn)Te system. Switching the TCI states on and off in bismuthene is much more straightforward, as shown in our proposed setups with tuning by substrates, pressure, and fields, which makes bismuthene an excellent candidate to realize the advantages of TCIs in achieving fast electronic switching via topological phase transitions, allowing for a high on/off ratio with low switching energy.

In the (Pb,Sn)Te system, changes in helicity upon applying an external electric field by activating the interaction between the surface Dirac cones have been reported in literature [47]. However, the breaking of the conducting edge channel is inevitable upon the application of electric field. In bismuthene, we have seen different behavior in our recent tight-binding studies of the edge spin texture [19]. Instead of eliminating the conducting edge channel, a moderate external electric field can lead to the formation of novel conducting spin edge transport channels protected by the interaction between the bulk and edge states. This observation potentially makes bismuthene a more versatile choice for edge state manipulation.

In summary, our results demonstrate the possibility of achieving a stabilized TCI phase in bismuthene and of controlling the TCI states via external factors. In addition, our tight-binding approach is transferable to other TCI materials. We believe this work will inspire further studies investigating the viability of TCIs in advanced electronic and spintronic applications.

3. Summary

Using a graphene-like bismuthene honeycomb as a representative 2D TCI, we have demonstrated that its edge states can be tuned in the following manner. Although it is well understood that mirror symmetry breaking substrate can open band gap, we show that choosing a substrate with weak interfacial interactions with TCI can still maintain the edge state. A bandgap can be opened by controlling the interfacial distance between the substrate and the monolayer. In such cases the interfacial distance acts as a switch to turn on and off the conduction channels, making it helpful for a switchable topological device with external applied pressure. Another approach is to maintain the edge states is via an edge band structure that does not have band crossing at generic k points. We have verified that the topological zigzag edge is maintained—while both changing interfacial distance and substrate effect leads to the change in a band shape, but does not lead to the opening of the band gap. We have also demonstrated that in a mirror-symmetry proteching substrate/bismuthene/substrate heterostructure, all edge states can survive despite changing the interfacial distance. The fact that TCI edge states are so vulnerable to one-sided substrates also encourages further studies in tuning the edge state structure with an electrical field. We have generalized the interaction using the mirror symmetry breaking Rashba term in an effective Hamiltonian and show that a ~120 meV band gap in the armchair edge can be opened with an effective electric field of 1.75 V/nm, indicating the effect can be generalized to mirror symmetry breaking terms for similar systems.

4. Methods

In all models considered in our study, we determined the topological electronic structure of bismuthene on a substrate using first principles calculations as implemented in Vienna Ab-Initio Simulation Package (VASP) [50,51]. The Perdew– Burke–Ernzerhof (PBE) [52] form of the generalized gradient approximation (GGA) [53] is used to describe electron exchange and correlation. The energy cut-off was set to at least

500 eV. All structures are fully relaxed until the ionic forces were less than 0.01 eV/Å. The vacuum was set to be at least 30 Å to avoid the interaction between periodic images. The h-BN and SiC(0001) substrates were modelled with 3 BN layers and 4 SiC layers. A dense 21 × 21 × 1 *kpoint* grid was used to sample the Brillouin zone for accurate calculations of electronic structures. Wannier90 code [54] was used to generate Wannier tight-binding Hamiltonians, which are extracted for the calculation of topological edge states. The Hamiltonians are constructed with bismuth p_x, p_y and p_z orbitals, with the effect of substrate incorporated into the model via downfolding method [55,56]. The software WANNIERTOOLS [57] was applied to perform edge states calculations based on iterative Green's function methods [29,58,59].

CRediT authorship contribution statement

Chutian Wang: Writing – review & editing, Writing – original draft, Visualization, Methodology, Investigation, Formal analysis, Data curation. **Yuefeng Yin:** Writing – review & editing, Supervision, Investigation, Conceptualization. **Thanh Tung Huynh:** Investigation, Writing – review & editing. **Michael S. Fuhrer:** Writing – review & editing, Supervision, Funding acquisition. **Nikhil V. Medhekar:** Writing – review & editing, Supervision, Funding acquisition, Conceptualization.

Declaration of competing interest

The authors declare that they have no known competing financial interests or personal relationships that could have appeared to influence the work reported in this paper.

Acknowledgements

All authors acknowledge funding support from the Australian Research Council Center for Excellence Future Low Energy Electronic Technologies (CE170100039). C.W. acknowledges support from Monash Graduate Scholarship. C.W., Y.Y., T.T.H. and N.V.M. gratefully acknowledge the support of computation resources from Australian National Computing Infrastructure and Pawsey Supercomputing Facility.

Appendix A. Supplementary data

Supplementary data to this article can be found online at https://doi.org/10.1016/j.mtphys.2025.101897.

Data availability

Data will be made available on request.

References

[1] Y.P. Feng, et al., Prospects of spintronics based on 2D materials, WIREs Comput. Mol.Sci. 7 (5) (2017) e1313.
[2] T. Senthil, Symmetry-protected topological phases of quantum matter, Annu. Rev. Condens. Matter Phys. 6 (1) (2015) 299–324.
[3] M.G. Vergniory, et al., A complete catalogue of high-quality topological materials, Nature 566 (7745) (2019) 480–485.
[4] Q. Liu, et al., Switching a normal insulator into a topological insulator via electric field with application to phosphorene, Nano Lett. 15 (2) (2015) 1222–1228.
[5] M. Nadeem, X. Wang, Spin gapless quantum materials and devices, Adv. Mater. 36 (33) (2024): 2402503.
[6] H. Sun, et al., Valley-dependent topological phase transition and quantum anomalous valley Hall effect in single-layer RuClBr, Phys. Rev. B 105 (19) (2022): 195112.
[7] S.-J. Zhang, et al., Intrinsic Dirac half-metal and quantum anomalous Hall phase in a hexagonal metal-oxide lattice, Phys. Rev. B 96 (20) (2017): 205433.
[8] Z. Zhang, et al., Magnetic quantum phase transition in Cr-doped $Bi_2(Se_xTe_{1-x})_3$ driven by the Stark effect, Nat. Nanotechnol. 12 (10) (2017) 953–957.
[9] A.C. Lygo, et al., Two-dimensional topological insulator state in Cadmium Arsenide thin films, Phys. Rev. Lett. 130 (4) (2023): 046201.
[10] J.L. Collins, et al., Electric-field-tuned topological phase transition in ultrathin Na_3Bi, Nature 564 (7736) (2018) 390–394.
[11] T. Zhang, et al., Electric-field tuning of the surface band structure of topological insulator Sb_2Te_3 thin films, Phys. Rev. Lett. 111 (5) (2013): 056803.
[12] J. Chen, et al., Topological phase change transistors based on tellurium Weyl semiconductor, Sci. Adv. 8 (23) (2022) eabn3837.
[13] A. Gao, et al., Layer Hall effect in a 2D topological axion antiferromagnet, Nature 595 (7868) (2021) 521–525.
[14] P. Bampoulis, et al., Quantum spin Hall states and topological phase transition in germanene, Phys. Rev. Lett. 130 (19) (2023): 196401.
[15] S.K. Chong, et al., Electrical manipulation of topological phases in a quantum anomalous Hall insulator, Adv. Mater. 35 (11) (2023): 2207622.
[16] L. Chen, Z.F. Wang, F. Liu, Robustness of two-dimensional topological insulator states in bilayer bismuth against strain and electrical field, Phys. Rev. B 87 (23) (2013): 235420.
[17] Y. Ando, L. Fu, Topological crystalline insulators and topological superconductors: from concepts to materials, Annu. Rev. Condens. Matter Phys. 6 (1) (2015) 361–381.
[18] J. Liu, et al., Spin-filtered edge states with an electrically tunable gap in a two-dimensional topological crystalline insulator, Nat. Mater. 13 (2013) 178–183.
[19] Y. Yin, et al., Extracting unconventional spin texture in two dimensional topological crystalline insulator bismuthene via tuning bulk-edge interactions, Materials Today Physics 36 (2023): 101168.
[20] K. Kobayashi, Electronic states of SnTe and PbTe (001) monolayers with supports, Surf. Sci. 639 (2015) 54–65.
[21] F. Reis, et al., Bismuthene on a SiC substrate: a candidate for a high-temperature quantum spin Hall material, Science 357 (6348) (2017) 287–290.
[22] R. Canyellas, et al., Topological edge and corner states in bismuth fractal nanostructures, Nat. Phys. 20 (2024) 1421–1428.
[23] L. Chen, et al., Exceptional electronic transport and quantum oscillations in thin bismuth crystals grown inside van der Waals materials, Nat. Mater. 23 (6) (2024) 741–746.
[24] S.-S. Li, et al., Effect of Amidogen functionalization on quantum spin Hall effect in Bi/Sb(111) films, ACS Appl. Mater. Interfaces 9 (47) (2017) 41443–41453.
[25] C.-H. Hsu, et al., The nontrivial electronic structure of Bi/Sb honeycombs on SiC (0001), New J. Phys. 17 (2) (2015): 025005.
[26] G. Li, et al., Theoretical paradigm for the quantum spin Hall effect at high temperatures, Phys. Rev. B 98 (16) (2018): 165146.
[27] S. Sun, et al., Epitaxial growth of ultraflat bismuthene with large topological band inversion enabled by substrate-orbital-filtering effect, ACS Nano 16 (1) (2022) 1436–1443.
[28] Y. Ding, Y. Wang, Electronic structures of reconstructed zigzag silicene nanoribbons, Appl. Phys. Lett. 104 (8) (2014): 083111.
[29] S. Zhang, et al., Ideal inert substrates for planar antimonene: h-BN and hydrogenated SiC (0001), Phys. Chem. Chem. Phys. 20 (36) (2018) 23397–23402.
[30] Y. Hu, et al., Sandwiched epitaxy growth of 2D single-crystalline hexagonal bismuthene nanoflakes for electrocatalytic CO_2 reduction, Nano Lett. 23 (22) (2023) 10512–10521.
[31] C.-H. Hsu, et al., Two-dimensional topological crystalline insulator phase in Sb/Bi planar honeycomb with tunable Dirac gap, Sci. Rep. 6 (2016): 18993.
[32] X. Hao, et al., Strain-engineered electronic and topological properties of bismuthene on SiC(0001) substrate, Nano Futures 3 (4) (2019): 045002.
[33] K. Yaegashi, et al., Selective fabrication of bismuthene and α-Bi on hydrogen-terminated SiC(0001), Langmuir 38 (44) (2022) 13401–13406.
[34] Y.A. Mezenov, et al., Metal–organic frameworks in modern physics: highlights and perspectives, Adv. Sci. 6 (17) (2019): 1900506.
[35] A.L. Araújo, et al., Topological nonsymmorphic ribbons out of symmorphic bulk, Phys. Rev. B 93 (16) (2016): 161101.
[36] A.V. Krukau, et al., Influence of the exchange screening parameter on the performance of screened hybrid functionals, J. Chem. Phys. 125 (22) (2006).
[37] M. Yankowitz, et al., Dynamic band-structure tuning of graphene moiré superlattices with pressure, Nature 557 (7705) (2018) 404–408.
[38] Q. Li, et al., Localized Wannier function based tight-binding models for two-dimensional allotropes of bismuth, New J. Phys. 23 (6) (2021): 063042.
[39] J.S. Kim, et al., Formation of Klein edge doublets from graphene monolayers, ACS Nano 9 (9) (2015) 8916–8922.
[40] I.K. Drozdov, et al., One-dimensional topological edge states of bismuth bilayers, Nat. Phys. 10 (9) (2014) 664–669.
[41] R. Yu, et al., Equivalent expression of Z_2 topological invariant for band insulators using the non-Abelian Berry connection, Phys. Rev. B 84 (7) (2011): 075119.
[42] C.L. Kane, E.J. Mele, Quantum spin Hall effect in graphene, Phys. Rev. Lett. 95 (22) (2005): 226801.
[43] J.H. Xu, et al., Tight-binding theory of the electronic structures for rhombohedral semimetals, Phys. Rev. B 48 (23) (1993) 17271–17279.
[44] Y.-Z. Jia, et al., Prediction of topological crystalline insulators and topological phase transitions in two-dimensional PbTe films, Phys. Chem. Chem. Phys. 19 (43) (2017) 29647–29652.
[45] Y. Tanaka, et al., Experimental realization of a topological crystalline insulator in SnTe, Nat. Phys. 8 (11) (2012) 800–803.
[46] A. Sulich, et al., Unit cell distortion and surface morphology diversification in a SnTe/CdTe(001) topological crystalline insulator heterostructure: influence of defect azimuthal distribution, J. Mater. Chem. C 10 (8) (2022) 3139–3152.
[47] Y. Gong, et al., Experimental evidence of the thickness- and electric-field-dependent topological phase transitions in topological crystalline insulator SnTe (111) thin films, Nano Res. 11 (11) (2018) 6045–6050.
[48] P. Sessi, et al., Robust spin-polarized midgap states at step edges of topological crystalline insulators, Science 354 (6317) (2016) 1269–1273.

[49] J. Liu, W. Duan, L. Fu, Two types of surface states in topological crystalline insulators, Phys. Rev. B 88 (24) (2013): 241303.
[50] G. Kresse, J. Hafner, *Ab initio* molecular-dynamics simulation of the liquid-metal–amorphous-semiconductor transition in germanium, Phys. Rev. B 49 (20) (1994) 14251–14269.
[51] G. Kresse, J. Furthmüller, Efficient iterative schemes for ab initio total-energy calculations using a plane-wave basis set, Phys. Rev. B 54 (16) (1996) 11169–11186.
[52] J.P. Perdew, K. Burke, M. Ernzerhof, Generalized gradient approximation made simple, Phys. Rev. Lett. 77 (18) (1996) 3865–3868.
[53] D.C. Langreth, J.P. Perdew, Theory of nonuniform electronic systems. I. Analysis of the gradient approximation and a generalization that works, Phys. Rev. B 21 (12) (1980) 5469–5493.
[54] A.A. Mostofi, et al., wannier90: a tool for obtaining maximally-localised Wannier functions, Comput. Phys. Commun. 178 (9) (2008) 685–699.
[55] I.V. Solovyev, Z.V. Pchelkina, V.I. Anisimov, Construction of Wannier functions from localized atomiclike orbitals, Phys. Rev. B 75 (4) (2007): 045110.
[56] E. Zurek, J. Autschbach, O.K. Andersen, Downfolding and N-ization of basis sets of slater type orbitals, AIP Conf. Proc. 963 (2) (2007) 1421–1424.
[57] Q. Wu, et al., WannierTools: an open-source software package for novel topological materials, Comput. Phys. Commun. 224 (2018) 405–416.
[58] D.J. Klein, Graphitic polymer strips with edge states, Chem. Phys. Lett. 217 (3) (1994) 261–265.
[59] W. Jaskólski, et al., Edge states and flat bands in graphene nanoribbons with arbitrary geometries, Phys. Rev. B 83 (23) (2011): 235424.